

;

Received in **Research in Astronomy and Astrophysics** manuscript no.
 (L^AT_EX: fs2.tex; printed on May 14, 2022; 21:36)

Key words: Galaxy:General — Galaxy:Formation

The influence of stellar objects mass distribution on their gravitational fields

Vladimir Stephanovich¹, Włodzimierz Godłowski¹, Monika Biernacka² and Błażej Mrzygłód¹

¹ Uniwersytet Opolski, Institute of Physics, ul. Oleska 48, 45-052 Opole, Poland; *stef@uni.opole.pl*

² Institute of Physics, Jan Kochanowski University, ul. Swietokrzyska 15, 25-406 Kielce, Poland

Abstract We study theoretically the influence of the astronomical objects masses randomness on the distribution function of their gravitational fields. We have shown that mass randomness does not change the non-Gaussian character of the gravitational fields distribution. At the same time, our results show that mass distribution alters the dependences of the mean angular momenta of galaxies and clusters on their richness. The specific form of above dependence is determined by the interplay of mass distribution and different assumptions made about cluster morphology. We trace the influence of masses distribution on the time evolution of stellar objects angular momenta in CDM and Λ CDM models. We also compare our theoretical predictions with results derived both from observational data and numerical simulations.

1 INTRODUCTION

As the gravitational fields are highly nonuniform during galaxies and their clusters formation, the distribution of former plays an important role. Moreover, the character of gravitational field distribution permits to discern the specific scenario of galaxies formation. The classical scenarios of such formation had been proposed quite long time ago (Peebles (1969), Zeldovich (1970), Sunyaev & Zeldovich(1972), Doroshkevich (1973), Shandarin(1974), Efstathiou & Silk(1983), Dekel (1985)) and dealt primarily with so-called Zeldovich pancake model (Zeldovich (1970)), based on large gravitating body (of the pancake shape, hence the name) mechanical instability without any randomness in gravitational fields of the constituents (Zeldovich (1970), Shandarin & Zeldovich (1989), Longair (2008)). The improved form of the above classical scenarios has been put forward more recently, see Shandarin et al (2012), Giahi-Saravani & Schäfer (2014) for relevant references. The presence or absence of the random gravitational field fluctuations contribute to the question about angular moment acquisition of galaxies and their structures in their formation stages. This may in principle permit to specify the most probable (among many other) scenario of the large stellar objects formation.

One of the natural sources of gravitational fields randomness is the masses distribution of stellar objects.

a priori given distribution function of masses $\tau(M)$ has been considered. In this paper, all characteristics of the stellar ensemble has been expressed through the different average powers of mass. The mass averaging had there been performed implicitly with the above function $\tau(M)$. In principle, such approach can be generalized to the averaging over quadrupole and higher multipole moments of galaxies in the spirit of the [Stephanovich & Godłowski \(2015\)](#). Although this effect may change some of the results quantitatively, we speculate that its overall influence will be rather faint. Next step has been done by [Press & Shechter \(1974\)](#), who considered the distribution function of stellar objects masses within the model of self-similar gravitational condensation. In this work, within the model of the expanding Universe in Friedmann cosmology, the stellar ensembles had been represented as a "gas" of self-gravitating masses, which can condense into aggregates which larger mass, forming finally very large clumpy objects. This model permits to derive the distribution of masses in the form

$$f(m) = A \left(\frac{m}{m_*} \right)^\alpha e^{-m/m_*}, \quad (1)$$

where A is a normalization constant, see below. Note that the explicit expression of Shechter function (1) has been listed in the work [Shechter \(1976\)](#) devoted to the luminosity distribution in galaxies. Below we will use function (1) for the calculation of the amended (on the mass distribution) distribution function of the gravitational fields and angular momenta. Using this function, we assume that the mass is proportional to the first degree of a luminosity: $m \sim L$. Below we give the arguments why possible nonlinearity $m \sim L^\gamma$ ($\gamma \neq 1$) will not change our results qualitatively.

In the present paper, we consider tidal interaction in the ensemble of galaxies and their clusters in a Friedmann-Lemaître-Robertson-Walker Universe with Newtonian self-gravitating dust fluid ($\rho = 0$) containing both luminous and dark matter. The commonly accepted model of such Universe is spatially flat homogeneous and isotropic Λ CDM model. The clumpy objects like galaxies and their clusters are formed in this as a result of almost scale invariant Gaussian fluctuations ([Silk \(1968\)](#), [Peebles & Yu \(1970\)](#), [Sunyaev & Zeldovich \(1970\)](#)). This assumption is the base of the so-called hierarchical clustering model ([Doroshkevich \(1970\)](#), [Dekel \(1985\)](#), [Peebles \(1969\)](#)). The models with non-Gaussian initial fluctuations have also been considered in [Bartolo et al \(2004\)](#). The non-Gaussian character of distribution function has been postulated there, rather then calculated. Such calculation has been presented in [Stephanovich & Godłowski \(2015\)](#), [Stephanovich & Godłowski \(2017\)](#), where the non-Gaussian distribution of gravitational fields and momenta were calculated using method of [Chandrasekhar \(1943\)](#). Here we generalize this calculation considering the masses distribution (1). Note that the calculations made in [Stephanovich & Godłowski \(2015\)](#), [Stephanovich & Godłowski \(2017\)](#) dealt with equilibrium situation only. To consider non-equilibrium situation, it is necessary to use the differential equations of Fokker-Planck type with so-called fractional derivatives ([Garbaczewski & Stephanovich \(2009\)](#), [Garbaczewski & Stephanovich \(2011\)](#)). In this case we can start from ubiquitous Gaussian distribution and arrive at non-Gaussian one as a result of primordial, fast time evolution. After it, the slower evolution, dictated by the Λ CDM scenario, takes place.

In hierarchical clustering approach, the large clumpy structures form as a result of gravitational interactions between smaller objects. In other words, the galaxies spin angular momenta arise as a result of

mentum is the result of tidal interaction with the entire environment, which occurs via interaction transfer from close to distant galaxies, see below. That is to say that our approach is the generalization of [Schäfer & Merkel \(2012\)](#), [Catelan & Theuns \(1996\)](#), [Catelan & Theuns \(1996a\)](#), [Lee & Pen \(2002\)](#), where the average tidal interaction with the entire environment has been considered. In the present work we perform the theoretical analysis of the influence of tidal interaction between astronomical objects on the larger (then initial constituents) structures formation. We do so with respect to the additional distribution of masses, obeying Shechter function (1). It turns out, that the mass distribution (1) does not change our main result ([Stephanovich & Godłowski \(2015\)](#), [Stephanovich & Godłowski \(2017\)](#)) that in the stellar systems with multipole (tidal) gravitational interaction, the distribution function of gravitational fields cannot be Gaussian. The crux of the matter here is a long-range character of Newtonian (and derived multipole) interaction between stellar objects. Such character implies that distant objects (like galaxies, their clusters and even dark matter haloes) still "feel each other", which is not the case for Gaussian distribution. The derived non-Gaussian distribution function allows to calculate the distribution of virtually any observables (like angular momentum) of the astronomical structures (not only galaxy clusters but smooth component like haloes, which mass dominate the total mass of the cluster, see [Kravtsov, Borgani \(2012\)](#)) in any (linear or nonlinear) Eulerian approach.

The relation between angular momentum of the galaxy clusters and their masses has also been investigated from the observational point of view. As generally galaxy clusters do not rotate [Hwang & Lee \(2007\)](#), [Tovmassian\(2015\)](#), the angular momentum of a cluster is primarily due to spins of member galaxies. Unfortunately, usually we do not know angular momenta of galaxies. So the orientations of galaxies are investigated instead ([Oepik\(1970\)](#), [Hawley & Peebles\(1975\)](#), see [Romanowsky & Fall\(2012\)](#), [Pajowska et al.\(2019\)](#) for present review), as it is assumed that the rotational axes of galaxies are normals to their planes. Such assumption seems to be quite reasonable at least for the spiral galaxies. As a result, stronger alignment of galaxies in a structure mean larger angular momentum of the latter.

The question is, if there are any realtion between the alignment and mass of the structures. General result of the previous papers is that we have not satisfactory evidence for galaxies alignment in less massive structures like groups and poor clusters. However, we observe the alignment of galaxies in rich clusters, see [Godłowski, 2011](#), [Pajowska et al.\(2019\)](#) for review. First results ([Godłowski, Szydłowski & Flin \(2005\)](#), [Aryal\(2007\)](#)) were qualitative only. Because of that, [Godłowski et al.\(2010\)](#), [Godłowski\(2012\)](#) investigated quantitatively the orientation of galaxies in the sample of 247 rich Abell cluster, using improved [Hawley & Peebles\(1975\)](#) method (see [Pajowska et al.\(2019\)](#) for latest review). In these papers, it was found that the alignment is present in the above sample. Moreover, galaxy orientation increased with numerosness of the cluster. However, the data was not sufficient both to resolve the question about the exact form of this relationship and for confirmation of the hypothesis that the angular momentum of the structure increases with time. This is the reason that we decide to extend our sample and compared observational results

2 THE FORMALISM

Similar to the papers [Stephanovich & Godłowski \(2015\)](#), [Stephanovich & Godłowski \(2017\)](#) we consider here the quadrupolar (tidal) interaction of the stellar objects

$$\mathcal{H} = -G \sum_{ij} Q_i m_j V(\mathbf{r}_{ij}), \quad V(\mathbf{r}) = \frac{1}{2} \frac{3 \cos^2 \theta - 1}{r^3}, \quad (2)$$

where G is the gravitational constant, Q_i and m_i are, respectively, the quadrupole moment and mass of i -th object, $r_{ij} \equiv |\mathbf{r}_{ij}|$, $\mathbf{r}_{ij} = \mathbf{r}_j - \mathbf{r}_i$ is a relative distance between objects while θ is the apex angle. The Hamiltonian function (2) describes the interaction of quadrupoles, formed both from luminous and dark matter, see [Stephanovich & Godłowski \(2017\)](#) for details.

To account for the mass distribution (1), we begin with the expression for characteristic function $F(\rho)$ of the random gravitational fields' distribution ([Stephanovich & Godłowski \(2015\)](#), [Stephanovich & Godłowski \(2017\)](#)).

$$F(\rho) = \int_V n(\mathbf{r}) \left[1 - \frac{\sin \rho E(\mathbf{r})}{\rho E(\mathbf{r})} \right] d^3 r. \quad (3)$$

In the spirit of the article of [Chandrasekhar \(1943\)](#), we rewrite the expression (3) in the form

$$F(\rho) = \int_{V,m} n(\mathbf{r}, m) \left[1 - \frac{\sin \rho E(\mathbf{r}, m)}{\rho E(\mathbf{r}, m)} \right] d^3 r dm, \quad (4)$$

where $n(\mathbf{r}, m)$ is the number density (concentration, proportional to probability, see below) of stellar objects (galaxies, their clusters and also dark matter halos) at the position \mathbf{r} with a mass m . As the average density at large scales can be well regarded as constant (slowly spatially fluctuating to be specific), see [Chandrasekhar \(1943\)](#), [Press & Shechter \(1974\)](#), the number density n in Eq. (4) can be well regarded to be independent on the coordinates, i.e. $n = n(m)$. In this case the expression (4) reads

$$F(\rho) = \int_{V,m} n(m) \left[1 - \frac{\sin \rho E(\mathbf{r}, m)}{\rho E(\mathbf{r}, m)} \right] d^3 r dm, \quad (5)$$

where

$$E(\mathbf{r}, m) = E_0 \frac{3 \cos^2 \theta - 1}{r^4}, \quad E_0 = \frac{1}{2} G Q, \quad Q \approx m R^2 \quad (6)$$

is the quadrupolar field [Stephanovich & Godłowski \(2015\)](#), m is the mass of a stellar object (like galaxy or cluster) and R is its mean radius. We take the function $n(m) \equiv f(m)$ in the form of the Shechter function (1), where m_* and α are adjustable parameters. We obtain the normalization constant A from the condition (see Eq. (4) of [Press & Shechter \(1974\)](#))

$$n = \int_0^\infty n(m) dm, \quad (7)$$

where n is our previous constant concentration [Stephanovich & Godłowski \(2015\)](#), [Stephanovich & Godłowski \(2017\)](#). Note, that there is no problem to take any other dependence $n(m)$ which will not complicate our consideration a lot. As we mentioned above, here we, following [Shechter \(1976\)](#), assume that the luminosity is directly proportional to the first degree of a mass $\tilde{L} \sim m$. But there is no problem to consider the higher degrees in this relation like $\tilde{L} \sim m^k$, $k = 4$. In this case, the

The explicit calculation gives

$$n = A \int_0^\infty \left(\frac{m}{m_*} \right)^\alpha e^{-m/m_*} dm = A m_* \Gamma(1 + \alpha). \Rightarrow A = \frac{n}{m_* \Gamma(1 + \alpha)}. \quad (8)$$

Here $\Gamma(z)$ is Euler Γ - function (Abramowitz & Stegun (1972)). Finally we have from (5)

$$F(\rho) = \frac{n}{m_* \Gamma(1 + \alpha)} \int_V \int_0^\infty dm \left(\frac{m}{m_*} \right)^\alpha e^{-m/m_*} \left[1 - \frac{\sin \rho E(\mathbf{r}, m)}{\rho E(\mathbf{r}, m)} \right] d^3 r, \quad (9)$$

where $E(\mathbf{r}, m)$ is given by the equation (6). It turns out that the equation (8) can be reduced to the Eqs (17) and (18) from Ref. Stephanovich & Godłowski (2015) but with slightly renormalized coefficient before $\rho^{3/4}$. This is because under the assumption that n does not depend on coordinates (it depends only on mass, see Eq. (1)), the coordinates and mass turn out to be effectively decoupled. To do so, we perform first the integration over $d^3 r$ in (8). This integration is exactly the same as that in Ref. Stephanovich & Godłowski (2015) (since the mass enters Eq. (6) through parameter E_0 which is unimportant for coordinate integration) so that we have from (9)

$$F(\rho) = 2\pi \cdot 0.41807255 \rho^{3/4} E_{10}^{3/4} \int_0^\infty m^{3/4} n(m) dm, \quad E_{10} = \frac{1}{2} G R^2. \quad (10)$$

The integral in (10) can be performed as follows

$$\begin{aligned} I &= \int_0^\infty m^{3/4} n(m) dm = \frac{n}{m_* \Gamma(1 + \alpha)} \int_0^\infty m^{3/4} \left(\frac{m}{m_*} \right)^\alpha e^{-m/m_*} dm = \\ &= \frac{n m_*^{7/4}}{m_* \Gamma(1 + \alpha)} \int_0^\infty x^{\alpha+3/4} e^{-x} dx = n m_*^{3/4} \frac{\Gamma(\alpha + \frac{7}{4})}{\Gamma(\alpha + 1)}. \end{aligned} \quad (11)$$

Finally

$$F(\rho) = 2\pi n m_*^{3/4} \frac{\Gamma(\alpha + \frac{7}{4})}{\Gamma(\alpha + 1)} E_{10}^{3/4} \cdot 0.41807255 \cdot \rho^{3/4} \equiv \kappa \rho^{3/4}, \quad (12)$$

where

$$\kappa = 2\pi n \cdot 0.41807255 \cdot E_0^{*3/4} \frac{\Gamma(\alpha + \frac{7}{4})}{\Gamma(\alpha + 1)}, \quad E_0^* \equiv m_* E_{10} = \frac{1}{2} G m_* R^2 \equiv \frac{1}{2} G Q^*. \quad (13)$$

The expressions (12), (13) give the answer for the case when we have Shechter distribution for galaxies masses. The difference between previous case (Stephanovich & Godłowski (2015), Stephanovich & Godłowski (2017)) of a single mass is that now the width of distribution function of random gravitational fields depends on the fitting parameters m_* and α . Note that for *any* function $n(m)$ the result for characteristic function $F(\rho)$ will be Ex. (12) but with different coefficient κ .

3 CALCULATION OF THE MASS DEPENDENCE OF MEAN ANGULAR MOMENTUM

To derive the mass dependence of mean angular momentum, we should first calculate the distribution function of gravitational fields $f(E)$, then using linear relation between angular momentum L and field E (here, without loss of generality, we consider the moduli of corresponding vectors, see Stephanovich & Godłowski (2015), Stephanovich & Godłowski (2017) for details), derive the distribution function $f(L)$, from which we obtain the desired dependence.

The expression for the field E distribution reads (Stephanovich & Godłowski (2015))

$$f(E) = \frac{1}{\rho} \int_{\rho}^{\infty} e^{-i E \rho - F(\rho)} d^3 r = \frac{1}{\rho} \int_0^\infty e^{-\kappa \rho^{3/4}} \sin \kappa E d \rho. \quad (14)$$

where $F(\rho)$ is the characteristic function (12). Function $f(E)$ is normalized as follows

$$4\pi \int_0^\infty E^2 f(E) dE = 1 \quad (15)$$

and coefficient κ is given by the expression (13). The distribution function of angular momenta can be expressed by usual way from above $f(E)$

$$f(L) = f[E(L)] \left| \frac{dE(L)}{dL} \right|. \quad (16)$$

This gives explicitly (see [Stephanovich & Godłowski \(2015\)](#), [Stephanovich & Godłowski \(2017\)](#))

$$f(\lambda) = \frac{I(\lambda)}{2\pi^2 \lambda^3 \kappa^4 L_0(t)}, \quad (17)$$

where $\lambda = L/(L_0(t)\kappa^{4/3})$,

$$I(\lambda) = \int_0^\infty x \sin x \exp \left[-\left(\frac{x}{\lambda} \right)^{3/4} \right] dx. \quad (18)$$

Function $L_0(t)$ defines the model (CDM or Λ CDM) used ([Stephanovich & Godłowski \(2017\)](#)).

3.1 CDM model

Equation (12) shows that the distribution function of angular momenta for the case of distributed masses is similar to that from Ref. [Stephanovich & Godłowski \(2015\)](#) with the only change $\alpha \rightarrow \kappa$. This means that the mean dimensionless angular momenta reads ([Stephanovich & Godłowski \(2015\)](#), [Stephanovich & Godłowski \(2017\)](#))

$$\lambda_{max} = 0.602730263. \quad (19)$$

Now we should express parameter κ through galaxy (but not cluster, which is steel equals to $M = mN$, where m is galaxy mass, M is cluster mass, N is a number of galaxies in a cluster, see Refs. [Stephanovich & Godłowski \(2015\)](#), [Stephanovich & Godłowski \(2017\)](#)) mass m . This quantity is now defined as an average mass with distribution (1)

$$m = \int_0^\infty m_1 n(m_1) dm_1 \equiv \frac{n m_*^2 \Gamma(\alpha + 2)}{m_* \Gamma(1 + \alpha)} = (\alpha + 1) m_* n. \quad (20)$$

The expression (20) implies that the galaxy mass m is related to the mass distribution parameter m_* as

$$m_* = \frac{m}{n(\alpha + 1)}. \quad (21)$$

The next step is to substitute the expression (21) to the expression (13) for κ and express it through galaxy mass m instead of m_* . We have from Ex. (13)

$$\kappa^{4/3} = \frac{m E_{10} n^{1/3}}{\alpha + 1} \left[2\pi \cdot 0.41807255 \cdot \frac{\Gamma(\alpha + \frac{7}{4})}{\Gamma(\alpha + 1)} \right]^{4/3}. \quad (22)$$

In CDM model, the function $L_0(t)$ has the form ([Stephanovich & Godłowski \(2017\)](#))

$$L_0(t) = \frac{2I}{3} \frac{t}{t_0^2}, \quad (23)$$

where $I \approx mR^2$ is a galaxy moment of inertia and t_0 is a time scale. We have from the equation (19) in dimensional units

$$L_{max} = \lambda_{max} L_0 \kappa^{4/3} \equiv 0.6027 \frac{2I}{3} \frac{t}{t_0^2} \frac{m E_{10} n^{1/3}}{1 + \alpha} \left[2\pi \cdot 0.418 \cdot \frac{\Gamma(\alpha + \frac{7}{4})}{\Gamma(\alpha + 1)} \right]^{4/3} \\ = 0.7281884 \frac{t}{t_0^2} \frac{m^2 n^{1/3}}{\zeta^{4/3} C P^4} \zeta = \frac{\Gamma(\alpha + \frac{7}{4})}{\zeta^{4/3}} \quad (24)$$

Comparison of the expression (24) with Ex. (12) from Ref. [Stephanovich & Godłowski \(2015\)](#) shows that their only difference is other power of n . Namely, while latter Ex. (12) involves $n^{4/3}$, our expression (24) contains $n^{1/3}$. This is the consequence of the star masses distribution according to the Shechter function. We note also that the above mass distribution leaves the power of galaxy mass m intact, i.e. both expressions involve m^2 . This gives that in the first scenario (see below and Eq. (13) of [Stephanovich & Godłowski \(2017\)](#)) the dependence of L_{max} on galaxy cluster mass $M = mN$ will be the same $\sim M^{5/3}$. At the same time, in the second scenario (Eq. (15) of Ref. [Stephanovich & Godłowski \(2017\)](#)) the dependence on M will be $M^{1/3}$ instead of $M^{4/3}$. We now derive the dependences on M within both scenarios of Ref. [Stephanovich & Godłowski \(2017\)](#).

3.1.1 First scenario

In this scenario we represent galaxy volume as $V = R^3$ ([Stephanovich & Godłowski \(2017\)](#)), where R is the mean radius of a galaxy. In this case we have from (24)

$$\begin{aligned} L_{max} &= \eta m^2 n^{1/3} R^4 = \eta m^2 R^4 \frac{N^{1/3}}{V^{1/3}} \equiv \eta m^2 R^4 \frac{N^{1/3}}{R} = \eta m^2 R^3 N^{1/3} = \\ &= \eta \frac{R^3}{N} M^{5/3} \frac{m^{1/3}}{N^{1/3}} = \eta \frac{1}{n} M^{5/3} \frac{\rho^{1/3}}{n^{1/3}} = \eta M^{5/3} \frac{\rho^{1/3}}{n^{4/3}}, \quad \eta = \frac{t}{t_0^2} \frac{0.728...G}{1+\alpha} \zeta^{4/3}, \quad \rho = \frac{m}{V}, \quad n = \frac{N}{V}. \end{aligned} \quad (25)$$

The comparison of Eq. (25) and Eq. (13) from Ref. [Stephanovich & Godłowski \(2017\)](#) shows that the $M^{5/3}$ is the same, but the galaxies concentration n now enters in the power 4/3 instead of 1/3. One more difference is that now Shechter exponent α (see Eq. (1)) enters the answer via parameters η and ζ . It should be extracted from the best fit between expression (25) and observational data.

3.1.2 Second scenario

In this scenario the galaxy volume is $V = R_A^3$, where R_A is a mean galaxy cluster radius. We have from (24)

$$\begin{aligned} L_{max} &= \eta m^2 n^{1/3} R^4 = \eta m^2 R^4 \frac{N^{1/3}}{R_A} = \eta \frac{R}{R_A} R^3 m^2 N^{1/3} = \\ &= \eta \frac{R}{R_A} R^3 m^2 \frac{M^{1/3}}{m^{1/3}} = \eta \frac{R}{R_A} R^3 m^{5/3} M^{1/3}. \end{aligned} \quad (26)$$

It is seen, that contrary to Eq. (15) of Ref. [Stephanovich & Godłowski \(2017\)](#), here we have $M^{1/3}$. Also, the Shechter parameter α enters the answer.

3.2 Λ CDM model

Here, similar to [Stephanovich & Godłowski \(2015\)](#), we should isolate the contribution from time dependent functions $f_{1,2}(\tau)$ ($\tau = t/t_0$, $t_0 = 2/(3H_0\sqrt{\Omega_\Lambda})$, see Ex. (46) of [Stephanovich & Godłowski \(2015\)](#)) and $i = 1, 2$ numbers the orders (first and second respectively) of perturbation theory. Following [Stephanovich & Godłowski \(2015\)](#), we have for argument of the distribution function $H(\lambda, t)$ (Eq. (44) of [Stephanovich & Godłowski \(2015\)](#))

$$\chi(\tau) = \frac{L}{\tau} - \frac{1}{\tau} \quad (27)$$

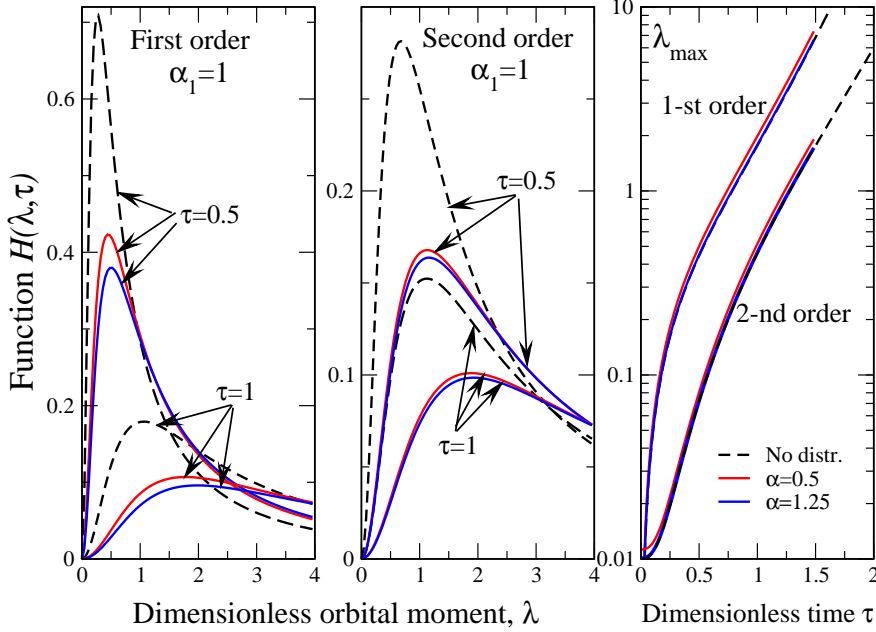


Fig. 1 Time evolution of the distribution function $H(\lambda, \tau)$ in Λ CDM model for the case of mass-dependent density (1). Left panel: first order of perturbation theory. Middle panel: second order. Right panel shows the dependence $\lambda_{max}(\tau)$ in the first and second orders of perturbation theory. In all panels, dashed lines (marked as "No distr." in the right panel) correspond to the previous case of mass-independent density n . We consider two Shechter exponents $\alpha = 0.5$ (red curves) and 1.25 (blue curves), coded by colors and explained in the legend in right panel. Parameter of Λ CDM model $\alpha_1 = \left(\frac{1-\Omega_\Lambda}{\Omega_\Lambda}\right)^{1/3} = 1$.

Similar to above CDM model, the maximum of the distribution function $\lambda_{max} = 0.602730263$ generates following relation

$$L_{max} = I\kappa^{4/3} \cdot 0.6027 f_i(\tau) \equiv \eta_{\Lambda CDMi}(\tau) m^2 R^4 n^{1/3},$$

$$\eta_{\Lambda CDMi}(\tau) = f_i(\tau) \frac{0.6027 \Psi^{4/3} G}{2(\alpha + 1)}, \quad \Psi = 2\pi \cdot 0.418 \cdot \frac{\Gamma(\alpha + \frac{7}{4})}{\Gamma(\alpha + 1)}. \quad (28)$$

The relation (28) is almost similar both in CDM and Λ CDM models. The only difference is in the functions $f_i(\tau)$, where in CDM model

$$f_1(\tau) = (2/3)\tau, \quad f_2(\tau) = (-4/3)\tau^{1/3}. \quad (29)$$

It is seen that the substitution of functions $f_{1,2}$ (29) yields immediately the expressions (25) and (26) for CDM model. In Λ CDM model the functions $f_{1,2}(\tau)$ should be taken from the solution of the differential equations (30) and (31) of [Stepanovich & Godłowski \(2015\)](#).

As the expression (28) for L_{max} is formally equivalent to Eqs (25) and (26), the dependences $L_{max}(M)$

The representative plots of the function $H(\lambda, \tau) = 2I(\lambda, \tau)/(\pi\lambda)$ (Stephanovich & Godłowski (2015)) and the maximal value $\lambda_{\max}(\tau)$ for the mass-dependent density (1) are reported in Fig. 1. Left and middle panels show the results for the first (Eq. (30) of Stephanovich & Godłowski (2015)) and second orders (Eq. (31) of Ref. Stephanovich & Godłowski (2015)) of perturbation theory. First, it is seen, that the distribution of masses does not make qualitative difference in the shape of distribution function. Namely, the shape of the dashed black curves (those without masses distribution) and red and blue ones is the same. At the same time, the distribution functions $H(\lambda, \tau)$ has substantially smaller amplitudes in the case of mass distribution. This means that the presence of mass distribution changes the functions $H(\lambda, \tau)$ quantitatively. The influence of Shechter exponent α Press & Shechter (1974), Shechter (1976) is minimal - the curves $H(\lambda, \tau)$ as well as $\lambda_{\max}(\tau)$ (right panel) are almost the same for $\alpha = 1.25$ and 0.5 , which is a big difference. This means that while the distribution of masses by itself changes the distribution function quantitatively, the value of constant α in that distribution is of minute influence. Our analysis shows that the above tendency persists for any time instant (in Fig. 1 we have only two time instants $\tau = 0.5$ and 1) and any reasonable $\alpha > 0$. The maximal values λ_{\max} are almost independent of the presence of mass distribution. Really, it is seen from right panel of Fig. 1, that both curves for no mass distribution (black dashed lines) and those with it lie very close to each other. This means simply that the physics of the system under consideration is determined by the distribution of random gravitational fields, than that of masses of stellar objects. May be the "full" dependence $n(\mathbf{r}, m)$ (4) (rather than present simplified situation $n(m)$ in each spatial point \mathbf{r} (5), (1)) will improve the situation. On the other hand, it is well acceptable that the robust distribution of gravitational fields simply do not changes qualitatively by small corrections like mass distribution. Latter, in turn, may mean, that next important step in the physics of galaxies formation is to consider the short-range interaction between galaxies (due to dark matter presence, for instance) so that the real average angular momentum (and not the distribution function maximum, considered so far) will appear, see Eq. (48) of Ref. Stephanovich & Godłowski (2015) and Eq. (28) of Ref. Stephanovich & Godłowski (2017).

4 OBSERVATIONAL DATA

First part of our data is the sample of rich Abell clusters containing at least 100 member galaxies each (Pajowska et al.(2019)). The sample contains 247 clusters and it was selected on the basis of the PF catalogue (Panko & Flin(2006)), see Pajowska et al.(2019) for details. However in the present paper we decide to restrict to 187 cluster which have directly obtained redshift. As our sample of PF clusters was not sufficient to confirm hypothesis that galaxies alignment decreases with redshift, we decide to enlarge our sample on the DSS base.

From ACO Catalogue (Abell, Corwin & Olowin (1989)) we selected all Abell clusters with galactic latitude $b > 40^\circ$ and richness class ≥ 1 . We obtained 1238 structures of galaxies from which we selected only those with redshifts $z < 0.2$ (Struble & Rood (1999)). Therefore, 377 clusters left for analysis. From DSS we extracted the area covering $2\text{Mpc} \times 2\text{Mpc}$ ($h = 0.75$, $q_0 = 0.5$) around each cluster. We applied the FOCAS package (Jarvis & Tyson (1981)) to the extracted regions and we obtained catalogues of galaxies, considering objects within the magnitude range $(m_3, m_3 + 3)$, where m_3 is the magnitude of the third bright-

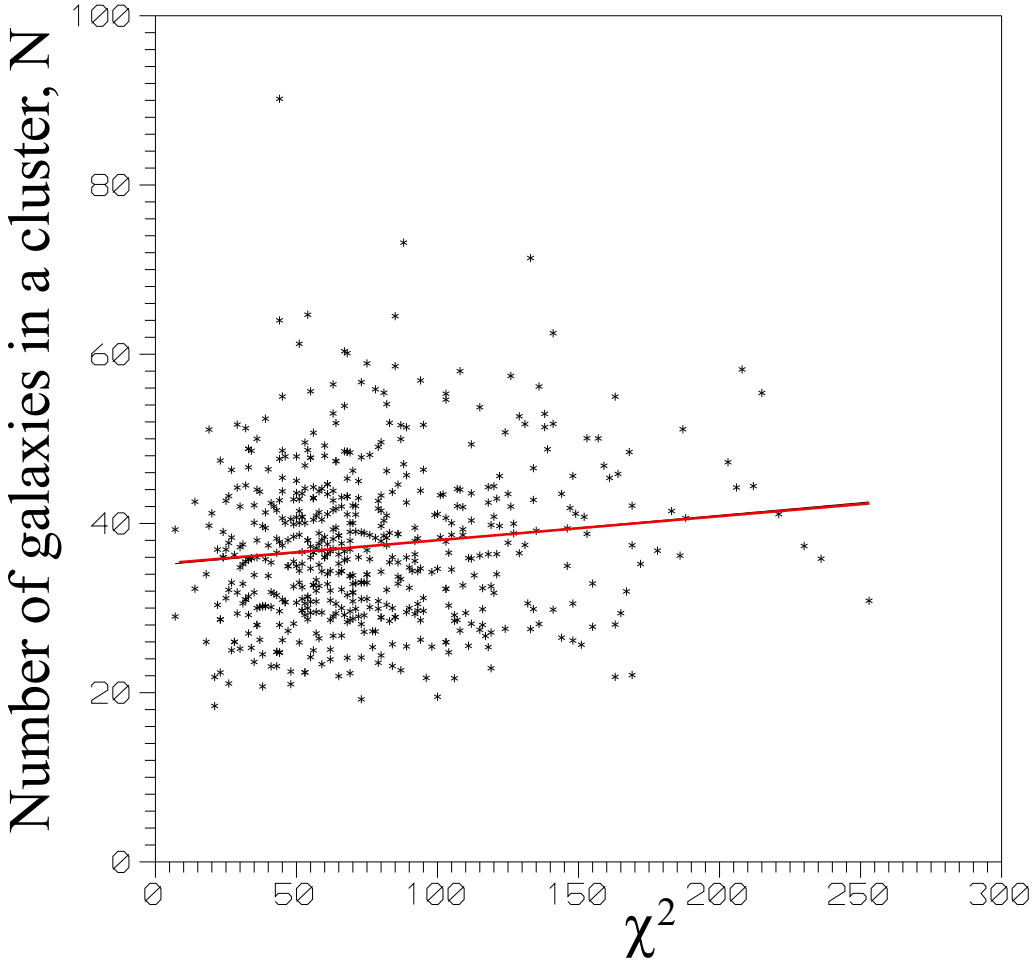


Fig. 2 Sample C. Relation between the number of galaxies in a cluster N and the value of analyzed statistics χ^2 .

incorrect star/galaxy classification. FOCAS calculates the catalogue parameters using the moments of pixel distribution in an object. There are three steps from the basic image to the object list in FOCAS: segmentation, area assembly and object evaluation. The various parameters characterizing the individual images in the segmented areas were calculated. In FOCAS the location of the object is defined by the centroids:

$$\bar{x} = \frac{1}{M_{00}} \sum_A x_i [I(x, y) - I_s] \quad (30)$$

$$\bar{y} = \frac{1}{M_{00}} \sum_A y_i [I(x, y) - I_s] \quad (31)$$

where M_{00} is zero moment, which is equal to:

$$M_{00} = \sum_A [I(x, y) - I_s] \quad (32)$$

The summation over A means that the sum includes all pixels in the object-defining area A . $I(x, y)$ is the intensity corresponding to the density at the location (x, y) in the digital plate image. I_s is the intensity corresponding to the average plate density at the object location. Shape information about the object is obtained from the higher central moments:

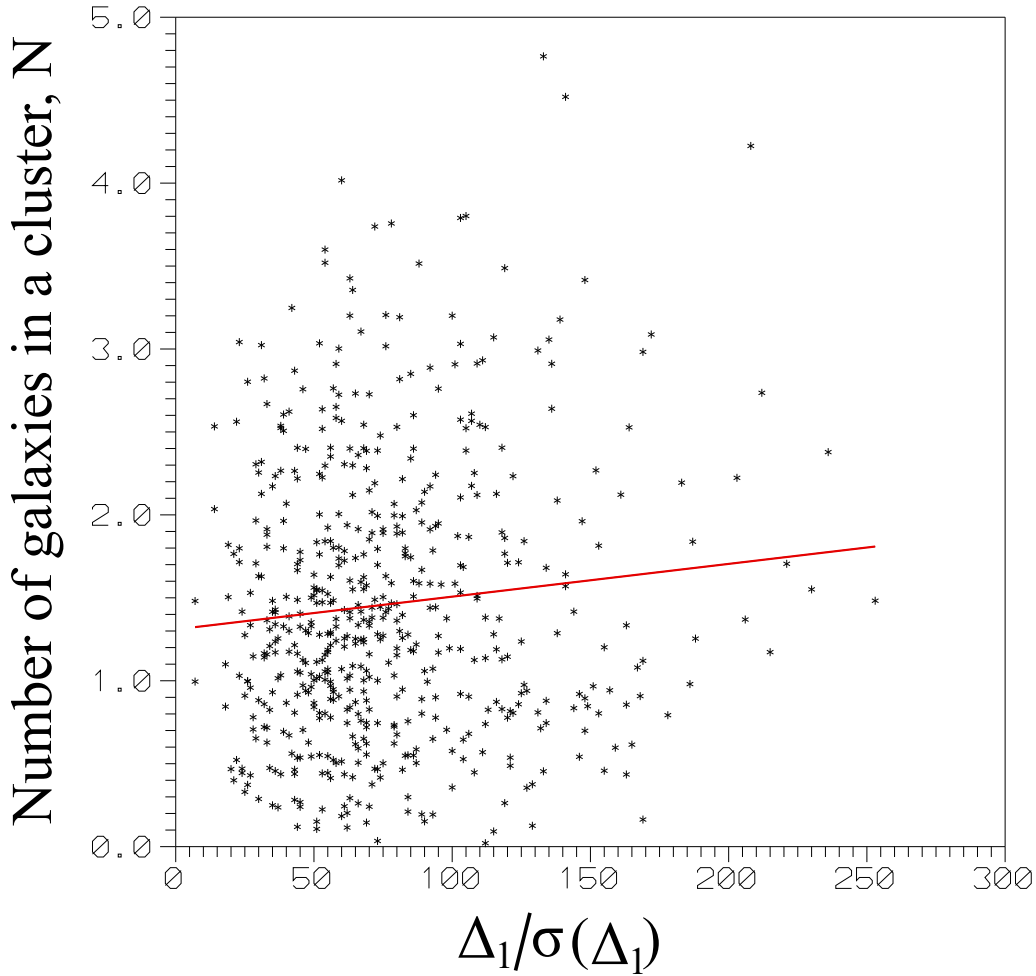


Fig. 3 Sample C. Relation between the number of galaxies in a cluster N and the value of analyzed statistics $\Delta_1/\sigma(\Delta_1)$.

The position angle of the object is calculated using central moments:

$$\tan(2\theta) = \frac{2M_{11}}{M_{20} - M_{02}} \quad (34)$$

Galaxy ellipticity reads

$$e = 1 - \frac{\lambda_2}{\lambda_1}, \quad (35)$$

where

$$\lambda_1^2 = \frac{1}{2} \left((M_{20} + M_{02}) + \sqrt{(M_{20} - M_{02})^2 + 4M_{11}^2} \right), \quad (36)$$

$$\lambda_2^2 = \frac{1}{2} \left((M_{20} + M_{02}) - \sqrt{(M_{20} - M_{02})^2 + 4M_{11}^2} \right), \quad (37)$$

Each catalogue contains information about the right ascension and declination of each galaxy, its coordinates x and y on the photographic plate, instrumental magnitude, object area, galaxy ellipticity and the position angle of the major axis of galaxy image. The equatorial galaxy coordinates for the epoch 2000 were computed according to the rectangular coordinates of DSS scans. We calculate the position angle and ellipticity of each galaxy cluster using the method described in Carter & Metcalfe (1980) which is also

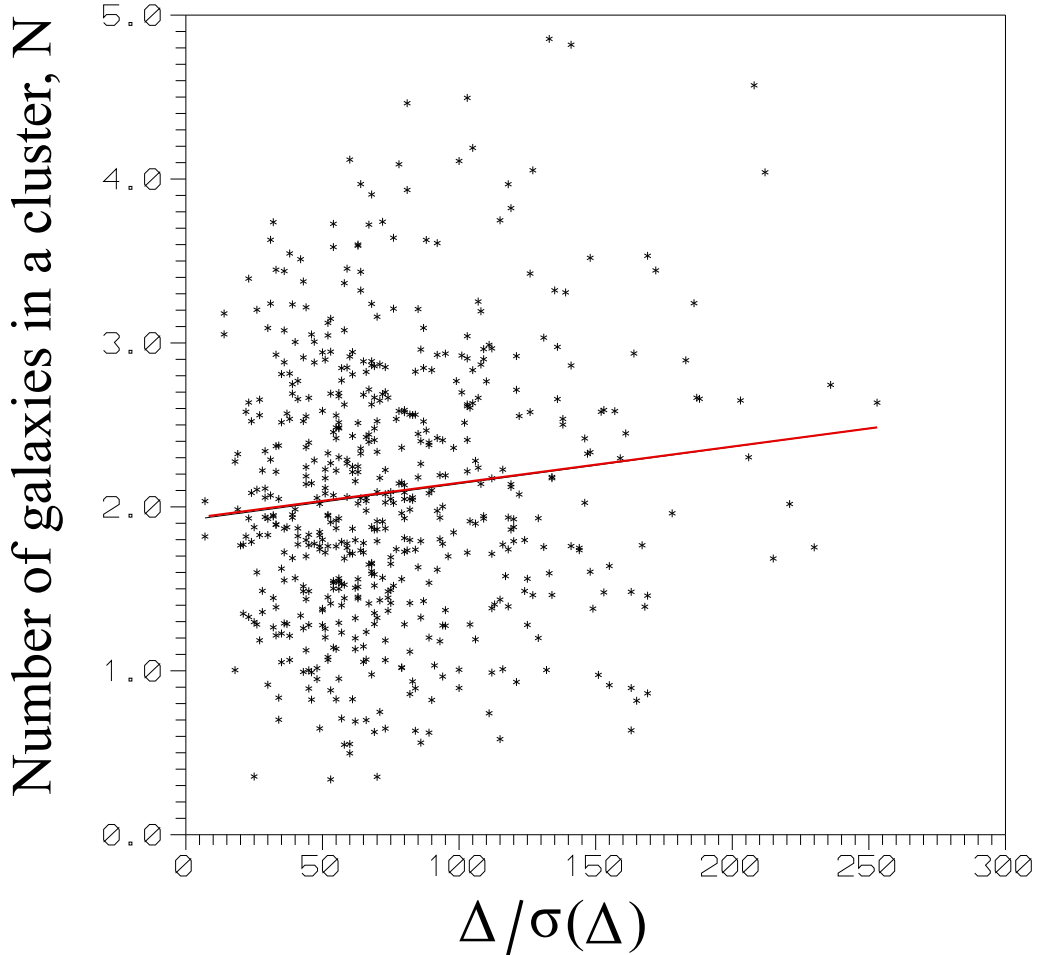


Fig. 4 Sample C. Relation between the number of galaxies in a cluster N and the value of analyzed statistics $\Delta/\sigma(\Delta)$.

5 STATISTICAL STUDIES

[Hawley & Peebles\(1975\)](#) propose to analyze the distribution of galaxies angular momenta by that of the observed position angles of the galactic image major axes. The direction of the angular momentum is then believed to be perpendicular to that of the major galaxy axis. This means that in the original version of the method the face-on and nearly face-on galaxies must be excluded from the analysis. This method can also be extended for the studies of the spatial orientation of galaxy planes ([Flin & Godłowski\(1986\)](#)).

The idea of [Hawley & Peebles\(1975\)](#) is to use the statistical tests for investigations of the position angles distribution. The higher value of statistics means greater deviation from isotropic distribution i.e. stronger alignment of galaxies angular momenta in the analyzed structures. Since [Hawley & Peebles\(1975\)](#) paper this method has become the standard tool for searching of galactic alignments. Recent improvement and revision of this method was presented in [Pajowska et al.\(2019\)](#).

In the present paper we follow the analysis from [Stephanovich & Godłowski \(2017\)](#). The entire range of investigated angles was divided into n bins. As the aim of the method is to detect non-random effect in the galaxies orientation, we first check if considered distribution deviates from isotropic one. Following

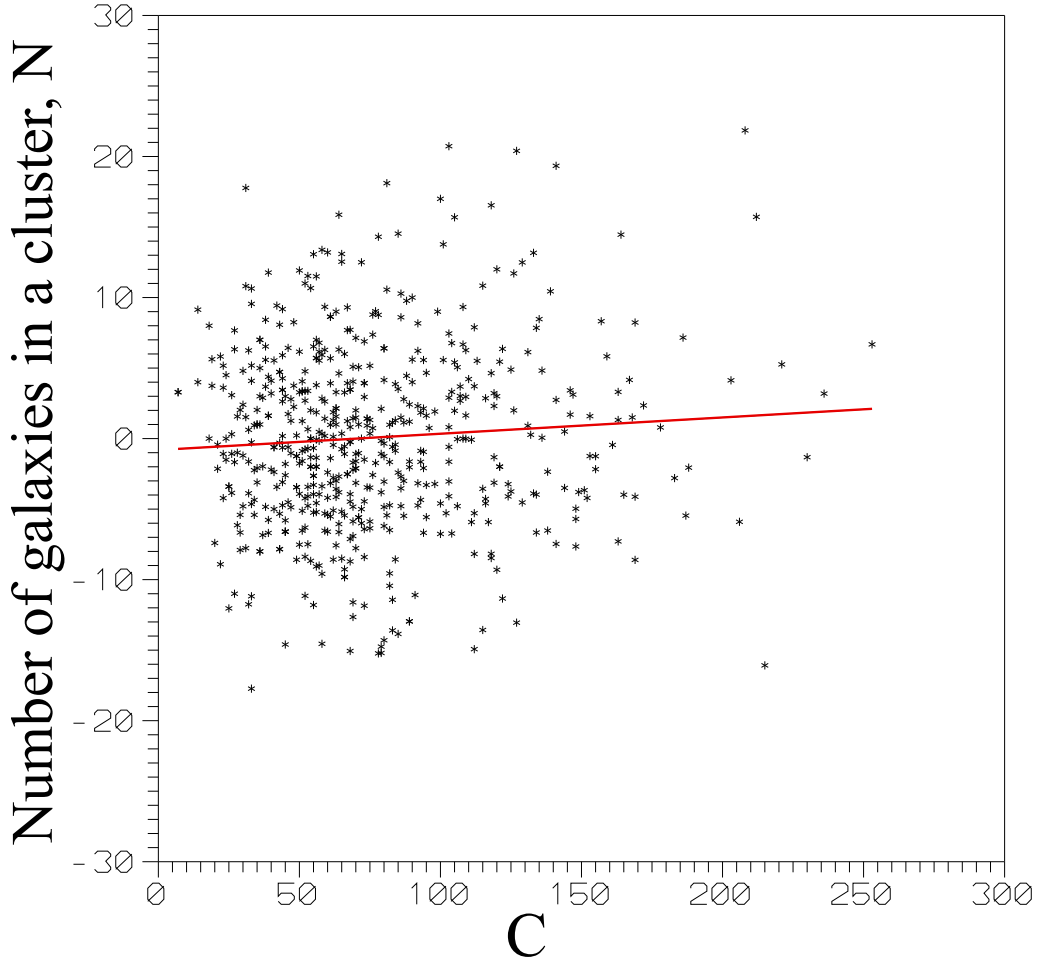


Fig. 5 Sample C. Relation between the number of galaxies in a cluster N and the value of analyzed statistics C .

analysis for first auto-correlation and Kolmogorov-Smirnov tests (K-S test) (Hawley & Peebles(1975), Flin & Godłowski(1986), Godłowski et al.(2010), Godłowski(2012) see Pajowska et al.(2019) for last review).

The statistics χ^2 is:

$$\chi^2 = \sum_{k=1}^n \frac{(N_k - N p_k)^2}{N p_k} = \sum_{k=1}^n \frac{(N_k - N_{0,k})^2}{N_{0,k}}, \quad (38)$$

where p_k are probabilities that chosen galaxy falls into k -th bin, N is the total number of galaxies in a sample (in a cluster in our case), N_k is the number of galaxies within the k -th angular bin and $N_{0,k}$ is the expected number of galaxies in the k -th bin.

The first auto-correlation test quantifies the correlations between galaxy numbers in neighboring angle bins. The statistics C reads

$$C = \sum_{k=1}^n \frac{(N_k - N_{0,k})(N_{k+1} - N_{0,k+1})}{[N_{0,k} N_{0,k+1}]^{1/2}}, \quad (39)$$

where $N_{n+1} = N_1$.

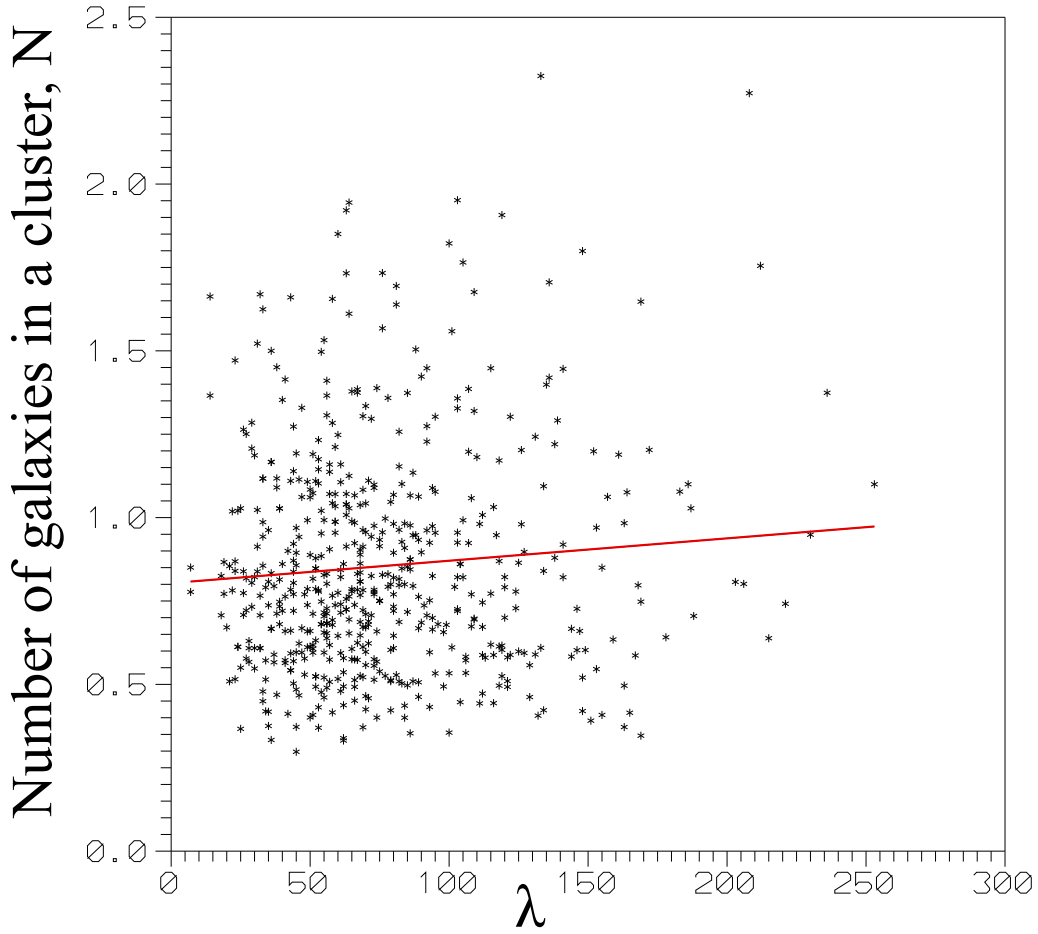


Fig. 6 Sample C. Relation between the number of galaxies in a cluster N and the value of analyzed statistics λ .

$$N_k = N_{0,k}(1 + \Delta_{11} \cos 2\theta_k + \Delta_{21} \sin 2\theta_k + \Delta_{12} \cos 4\theta_k + \Delta_{22} \sin 4\theta_k + \dots). \quad (40)$$

In this test, the statistically important are the amplitudes

$$\Delta_1 = (\Delta_{11}^2 + \Delta_{21}^2)^{1/2}, \quad (41)$$

(only the first Fourier mode is taken into account) or

$$\Delta = (\Delta_{11}^2 + \Delta_{21}^2 + \Delta_{12}^2 + \Delta_{22}^2)^{1/2}, \quad (42)$$

where the first and second Fourier modes are analyzed together. We investigate the statistics $\Delta_1/\sigma(\Delta_1)$ and $\Delta/\sigma(\Delta)$ (see Godłowski et al.(2010), Godłowski(2012), Pajowska et al.(2019) for details).

In the case of K-S test, the statistics under study is λ :

$$\lambda = \sqrt{N} D_n \quad (43)$$

which is given by limiting Kolmogorov distribution, where

$$D_n = \sup |F(x) - S(x)| \quad (44)$$

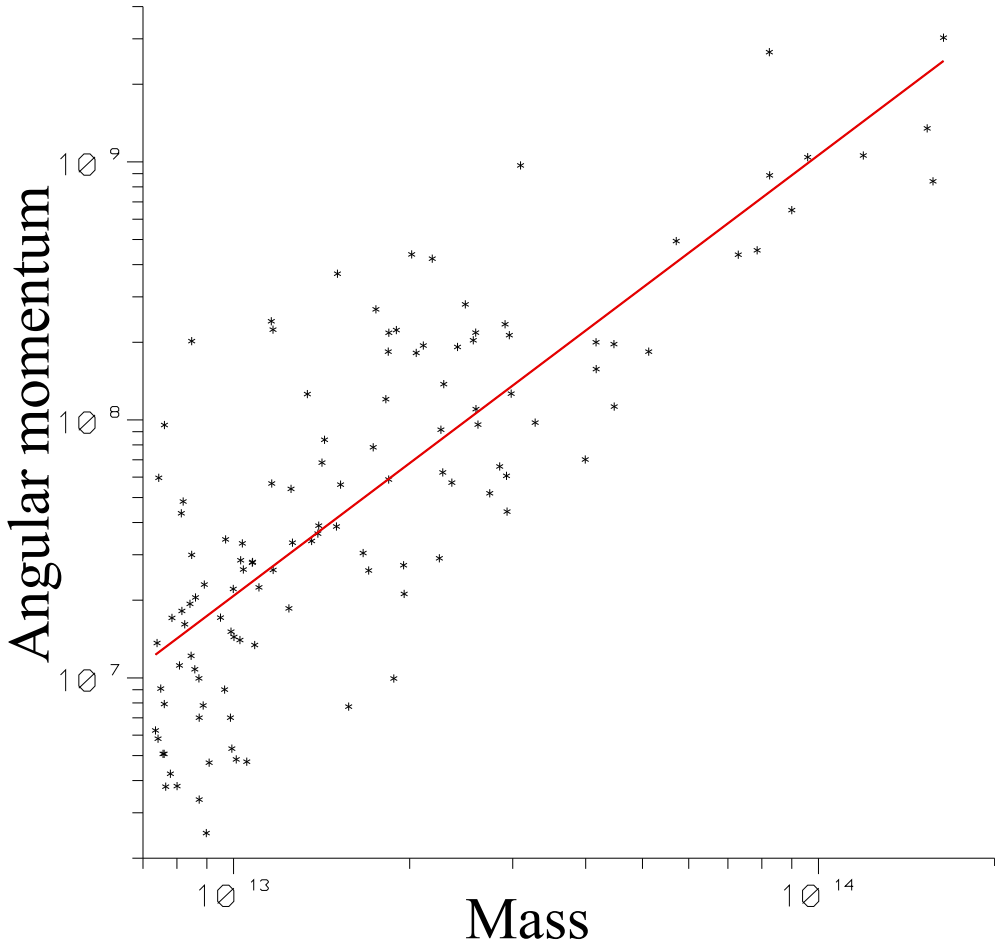


Fig. 7 Relation between angular momentum and mass of a cluster - Illustris simulation (Mass $> 10^{13}$ Solar Mass)

Using extended [Hawley & Peebles\(1975\)](#) method it is possible to analyze both the alignment dependence on particular parameter like richness of galaxy cluster [Godłowski et al.\(2010\)](#) and quantitatively answer the question if alignment is present in a sample (see [Pajowska et al.\(2019\)](#) for lat revision). In our previous papers [Godłowski et al.\(2010\)](#), [Stephanovich & Godłowski \(2017\)](#), using sample of 247 PF rich Abell clusters, it was shown that alignment of galaxies in a cluster increases significantly with its richness. Unfortunately available data was insufficient for persuasive conclusion about correctness of theoretically predicted [Stephanovich & Godłowski \(2015\)](#), [Stephanovich & Godłowski \(2017\)](#) dependence of analyzed statistics on redshift z .

For this reason we perform the investigations of our samples of galaxy clusters checking if there is a significant dependence between analyzed statistics and both richness and redshifts of the clusters. As a first step we analyzed the linear model $Y = aX + b$. The Y are the values of analyzed statistics i.e. χ^2 , $\Delta_1/\sigma(\Delta_1)$, $\Delta/\sigma(\Delta)$, C and λ (see [Stephanovich & Godłowski \(2017\)](#) for details) while X is the number of analyzed galaxies in each particular cluster or its redshift z respectively. Our null hypothesis H_0 is that analyzed statistics Y does not depend on X . This means that we should analyze the statistics $t = a/\sigma(a)$, which has Student's distribution with $u - 2$ degrees of freedom, where u is the number of analyzed

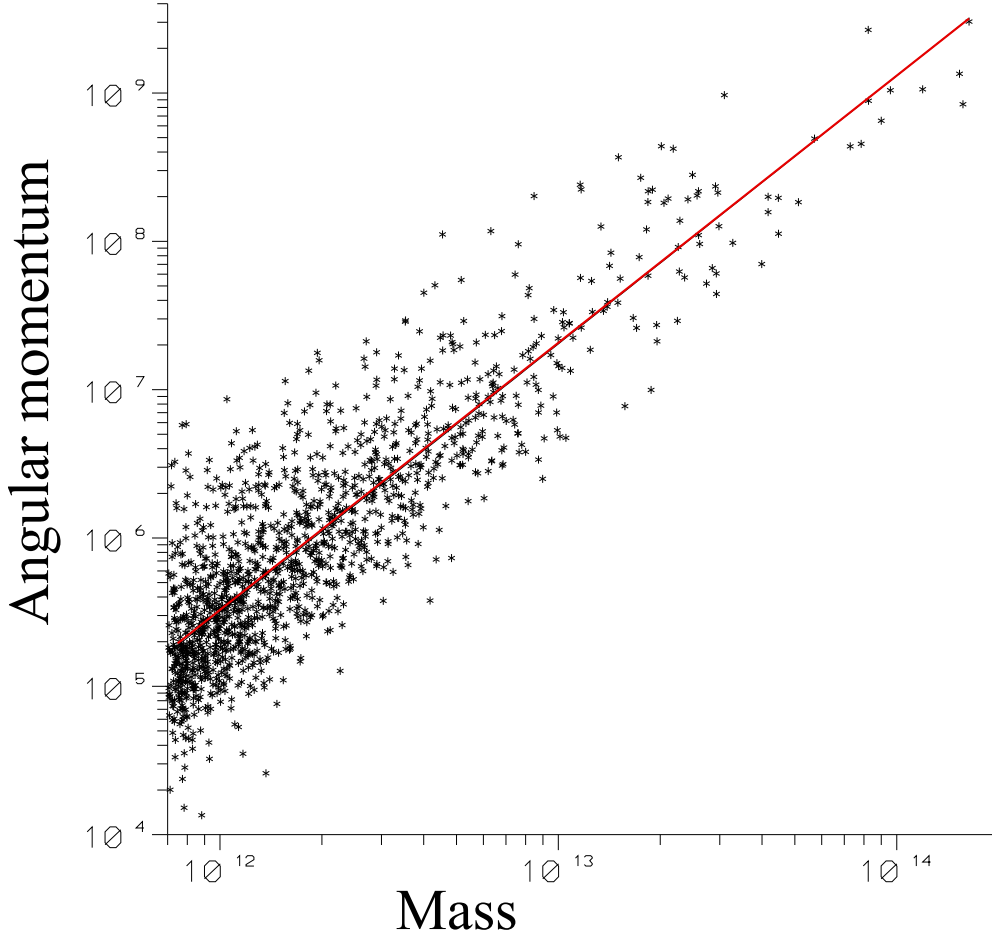


Fig. 8 Relation between angular momentum and mass of a cluster - Illustris simulation (Mass $> 10^{13}$ Solar Mass)

corresponds to the case of dependence on number of member galaxies in clusters and $t < 0$ to the case of dependence on redshift z . In order to reject the H_0 hypothesis, the value of observed statistics t should be greater than t_{cr} which could be obtained from the tables. For example, for sample 247 analyzed in [Stephanovich & Godłowski \(2017\)](#) at the significance level $\alpha = 0.05$, the value $t_{cr} = 1.651$.

The results are presented in the tables and figs 2-6. One could discern from the table 1, that while the analysis of the sample of 247 PF rich Abell clusters confirm the alignment increasing with cluster richness, then any test confirm nonzero deviation of linear regression parameter from zero. However, both above dependencies can be confirmed from the full sample (564 clusters) analysis. At first we conclude that analyzed statistics i.e. alignment, is significantly increasing with richness of a cluster, which confirms the result obtained in [Godłowski et al.\(2010\)](#), [Stephanovich & Godłowski \(2017\)](#) as well as theoretical prediction [Stephanovich & Godłowski \(2015\)](#). The details are also presented in the figures 1-5. Moreover, we could conclude that alignment decreases with z , which means that it increases with time as predicted by [Stephanovich & Godłowski \(2015\)](#), [Stephanovich & Godłowski \(2017\)](#).

However advanced look on the results show that situation is not so clear jet. This is because in real data usually the cluster richness decreases also with the redshift z . Quantitatively, in linear model, the

Table 1 The statistics $t = a/\sigma(a)$ for our sample of Abell clusters. Sample A - 247 rich Abell clusters from PF catalogue (as in [Stephanovich & Godłowski \(2017\)](#)). Sample B - full sample of 564 clusters (directly known redshift)

Test	$S = f(N)$	$S = f(z)$
Sample A		
χ^2	1.872	-0.769
$\Delta_1/\sigma(\Delta_1)$	1.613	0.611
$\Delta/\sigma(\Delta)$	1.964	-0.066
C	1.352	1.343
λ	2.366	0.176
Sample B		
χ^2	3.402	-2.342
$\Delta_1/\sigma(\Delta_1)$	2.857	-1.452
$\Delta/\sigma(\Delta)$	3.142	-1.646
C	1.825	-1.305
λ	2.333	-1.953

Table 2 The statistics $t = a/\sigma(a)$ for 3D analysis of our sample of Abell clusters. Sample B - full sample of 564 clusters (directly known redshift)

Test	$S = f(N)$	$S = f(z)$
Sample B		
χ^2	2.846	-1.434
$\Delta_1/\sigma(\Delta_1)$	2.250	-0.718
$\Delta/\sigma(\Delta)$	2.625	-0.811
C	1.538	-0.814
λ	2.000	-1.302

Table 3 The Illustris relation between Angular Momentum and mass simulations

Mass	a	σa	$t = a/\sigma a$
$> 10^{12}$	1.807	0.028	66.93
$> 10^{13}$	1.708	0.114	14.94

of t statistics $t = -7.066$. This is the reason that we repeated our analysis as 3D model $Y = a_1*N + a_2*z + b$. Note that until now such 3D analysis has not been performed in galaxies alignment studies, but because of the above reason, we consider it to be necessary here. In this extended analysis, the test statistics t are given by formulae $t_1 = a_1/\sigma(a_1)$ and $t_2 = a_2/\sigma(a_2)$. From Table 2, we could confirm that alignment increases significantly with cluster richness. One should note that all our tests show that statistics are decreasing with z , however values of t statistics are too small to make statistically significant (significance level $\alpha = 0.05$) effect.

6 SIMULATIONS

The [Illustris Project \(2018\)](#) was the simulation basis of our study. The Project used the AREPO code for

sumes a Λ CDM cosmology with the $\Omega_m = 0.2726$, $\Omega_\Lambda = 0.7274$, $\Omega_b = 0.0456$, $\sigma_8 = 0.809$, $n_s = 0.963$, and $H_0 = 100 \cdot h \cdot km \cdot s^{-1} Mpc^{-1}$ with $h = 0.704$. It contains multiple resolution runs with the highest resolution performed for Illustris - 1. Three different physical configurations was applied: dark matter only, non-radiative and full galaxy formation physics. In the case of the dark matter only simulations the mass was treated as collisionless. The non-radiation configuration also adds gas hydrodynamics, but ignores radiative cooling and star formation processes. The full galaxy formation physics contains (in addition to the previously mentioned ones) also processes related to galaxy formation through a model described in [Vogelsberger et al. \(2013\)](#). Illustris-1 consists of 136 runs for different redshifts z where the initial conditions was generated at $z = 127$ for snapshot 0 and evolved to $z = 0$ for snapshot 135.

Illustris successfully follows the coevolution of dark and visible matter. Haloes, subhaloes, and their basic properties have been identified with the FOF and SUBFIND algorithms ([Davis et al. \(1985\)](#), [Springel et al. \(2001\)](#), [Dolag et al. \(2009\)](#)), at each of the 136 stored snapshots. We've added information from the supplementary catalog to the resulting directory of Halos from [Zjupa & Springel \(2017\)](#). The code was written in such manner that it can run both as a postprocessing option to increase existing catalogues or as part of the regular group finding.

From Illustris - 1 we select Haloes at $z = 0$. We obtained 119 Haloes with total mass exceeding $10^{13} M_\odot$ and 1435 with total mass higher than $10^{12} M_\odot$. The angular momentum parameter for extracted Haloes was taken from [Zjupa & Springel \(2017\)](#).

Illustris simulations give direct value of both mass of the structures and their angular momentum. Present available data from Illustris are evolved to $z = 0$, so it is possible to study the dependence of angular momentum as the function of cluster mass but unfortunately not of redshift. However as we know directly the cluster angular momentum, it is not necessary to assume the linear relation between angular momentum and mass. Since theoretical modeling predicts usually the power low relations (see also [Stephanovich & Godłowski \(2015\)](#) for review) we could study the model $J = b \cdot M^a$. The latter relation could easily be rendered as a linear model $\ln J = \ln b + a \ln M$.

The results of the analysis are presented in the table 3 and figs 7 and 8. Analysis of ilustris simulation confirms that angular momentum of the cluster increases with its mass. In this case, the coefficient $a = 1.807 + / - 0.028$. The analysis of a sample of only the most massive clusters (mass $M > 10^{13}$ solar mass) gives $a = 1.708 + / - 0.114$ which is close to most popular theoretical prediction $a = 5/3 \approx 1.667$ (see [Godłowski et al.\(2010\)](#), [Stephanovich & Godłowski \(2017\)](#) for details).

7 OUTLOOK

In the present paper we have shown that the distribution of masses of the stellar objects does not alter substantially the distribution function of their gravitational fields. This shows that the main contribution to latter distribution function comes from the long-range Newtonian interaction between astronomical objects rather then from the distribution of their masses. At the same time, the mass distribution alters the dependence of L_{max} on astronomical objects concentration n (see Eq. (25)) and total cluster mass M (see Eq. (26)) , which may be observationally important. To discern, which of the dependences (25) or (26) is realized in

and dark matter components, one can ask a question about alignment of sub-dominant galaxies, even though the majority of galaxy clusters angular momenta is related to the smooth dark matter halo component. This question becomes important in view of the fact that mass distribution (1) alters the dependence on total cluster mass M (26). Namely, in the halo model (Schneider & Bridle (2010)), where the galaxies are embedded in a dark matter halo, latter may mediate the intergalaxy interaction, adding possible short-range terms to it. That is to say, to "see each other" in a dark matter halo, the galaxies should go closer to each other then in an empty space.

Note, that the observational results about lack of alignment of galaxies for less clumpy (so called poor) clusters, as well as evidence for such alignment in the clumpy (rich) ones (Godłowski, Szydłowski & Flin (2005), Aryal(2007), see also Godłowski, 2011 for incremental study and relevant references) clearly shows that angular momentum of galaxy groups and clusters increases with their mass (richness). The generalized analysis, based on Eq. (4), where $n = n(r, m)$ (i.e. the mass becomes spatially distributed), will improve the overall understanding, which can additionally be tested against observed galaxy shape distributions and alignments. The problem of angular momenta alignment due to their interactions as well as those with dark matter haloes has been simulated by Hahn et al. (2007). The main effect there is the presence of a threshold cluster mass (richness) value. Latter is related to mutual alignment of clusters and dark matter haloes axes. This fact can be analysed on the base of more general (then (1)) model (4). We postpone the consideration of this interesting question for the future publications.

Our formalism permit studying this effect (see Stephanovich & Godłowski (2017)) as well as the nonequilibrium time evolution of luminous astronomical objects (with respect to dark matter haloes) within the Λ CDM model. The combination of stochastic dynamical approaches (Garbaczewski & Stephanovich (2009), Garbaczewski & Stephanovich (2011)) along with deterministic one defined in Λ CDM model, may permit to answer (at least qualitatively) the question about the galaxies (and their clusters) initial alignment at the time of their formation. The interesting questions about how dark matter haloes influence (mediate) latter alignment, can also be answered within the above dynamic approach.

Our statistical analysis of sample of Abell clusters show that alignment of galaxies and their clusters angular momenta increases substantially with cluster mass. This result is confirmed also by 3D analysis, consisting in the studies of the dependence of galaxies alignment in a cluster both on cluster richness and redshift. We have also found that alignment decreases with redshift i.e. increases with time, but above 3D studies show that this effect is too faint to be confirmed statistically at the significance level $\alpha = 0.05$. Probable reason is that the corresponding relaxation time is too long. So for future investigations more extended data containing larger number of galaxy clusters (and with higher redshifts) are required. Analysis of the Illustris simulation also confirms the increase of galaxies angular momenta with cluster mass. Our studies favor the power law relation with coefficient 5/3 (i.e the value favored by most popular theoretical predictions - see, for instance, Stephanovich & Godłowski (2015), Stephanovich & Godłowski (2017)).

Let us finally note, that in the light of classical scenarios of galaxy formation, our results are in conformity with commonly preferred model of the galaxies formation, i.e. so-called hierachic clustering model

References

Abramowitz, M., Stegun, I., 1972, Handbook of Mathematical Functions with Formulas, Graphs, and Mathematical Tables (New York: Dover).

Aryal, B., Paudel, S., Saurer, W., 2007, MNRAS, 379, 1011

Bartolo, N., Komatsu, E., Matarrese, S., Riotto, A., 2004, Phys. Rep. 402, 103

Catelan, P., Theuns, T., 1996, MNRAS, 282, 436

Catelan, P., Theuns, T., 1996, MNRAS, 282, 455

Chandrasekhar, S., 1943, Rev. Mod. Phys., 15, 1

Dekel, A. 1985, ApJ, 298, 46

Doroshkevich, A. G. 1970, Astrofizika, 6, 581

Doroshkevich, A. G. 1973, ApJ, 14, 11

Efstathiou, G. A., Silk, J., 1983, The Formation of Galaxies, Fundamentals of Cosm. Phys. 9, 1

Garbaczewski, P., Stephanovich, V. A., 2009, Phys. Rev. E, 80, 031113

Garbaczewski, P., Stephanovich, V. A., 2011, Phys. Rev. E, 84, 011142

Giahi-Saravani, A., Schäfer, B.M. 2013 MNRAS, 437, 1847

Godłowski, W., Szydłowski, M., Flin, P. 2005, Gen. Rel. Grav. 37, (3) 615

Godłowski, W., 2011, IJMPD, 20, 1643

Hahn, O., Carollo, C.M., Porciani, C., Dekel, A., 2007, MNRAS, 381, 41

Kravtsov, A.V., Borgani, S., 2012, ARA&A, 50, 353

Lee, J., Pen, U. 2002, ApJ, 567, L111

Longair, M.S., 2008, Galaxy Formation. (Springer Berlin, Heidelberg, New York)

Peebles, P.J.E., 1969, ApJ, 155, 393

Peebles, P.J.E., Yu, J., T. 1970, ApJ, 162, 815

Press, W. and Shechter, P. 1974, ApJ, 187, 425

Schäfer, B. M., 2009, Int. J. Mod. Phys., 18, 173

Schäfer, B. M., Merkel, P. M., 2012, MNRAS, 421, 2751

Shandarin, S.F. 1974, Sov. Astr. 18, 392

Shandarin, S. F., Zeldovich, Ya. B., 1989 Rev. Mod. Phys. 61, 185

Shandarin, S.F., Habib, Sa., Heitmann, K., 2012, Phys. Rev. D, 85, 3005

Silk, J. 1968, ApJ, 151, 459

Shechter, P., 1976, ApJ, 203, 297

Schneider, M.D., Bridle, S., 2010, MNRAS, 402, 2127

Stephanovich, V.A., Godłowski, W., 2015, ApJ, 810, 167

Stephanovich, V.A., Godłowski, W., 2017, Research in Astron. Astrophys. (RAA), 17, 119

Sunyaev, A. R., Zeldovich, Ya. B., 1970, Astroph. Sp. Sci., 7, 3

Sunyaev, A. R., Zeldovich, Ya. B., 1972 A&A, 20, 189

Zeldovich, Ya. B., 1970, A&A, 5, 84

Abell G., Corwin H., Olowin R., 1989, AJSS, 70, 1

Aryal, B., Paudel, S., Saurer, W., 2007, MNRAS, 379, 1011

Carter D., Metcalfe N., 1980, MNRAS, 191, 325

Davis M., Efstathiou G., Frenk C. S., White S. D. M., 1985, ApJ, 292, 371

Dolag, K., Borgani, S., Murante, G., Springel, V. 2009, MNRAS, 399, 497

Flin, P., Godłowski, W. 1986, MNRAS, 222, 525

Godłowski, W., 2012, ApJ, 747, 7

Godłowski, W., Piwowarska, P., Panko, E., Flin, P., 2010, ApJ, 723, 985

Hawley, D. I., Peebles P. J. E., 1975, AJ, 80, 477

Hwang, H. S., Lee M. G., 2007, ApJ, 662, 236

Illustris Project <http://www.illustris-project.org>

Jarvis, J., Tyson, J., 1981, AJ 86, 476

Oepik, E. J., 1970, Irish AJ, 9, 211

Pajowska, P., Godłowski, W., Zhu Z. H., Popiela, J., Panko, E., Flin, P., 2019, JPAC, 02, 005,

Panko, E., Flin, P., 2006, J. of Astronomical Data, 12, 1

Springel, V., White, S. D. M., Tormen, G., Kauffmann, G., 2001, MNRAS, 328, 726-750
Springel, V. 2010, MNRAS, 401, 791
Struble M., Rood H., 1999, AJSS, 125, 35
Tovmassian, H. M., 2015, Astrophysics, 58, 471
Vogelsberger, M., Genel, S., Sijacki, D., et al. 2013, MNRAS, 436, 3031
Zjupa, J., Springel, V., 2017, MNRAS, 466, 1625-1647